On a Alvenicity of solar wind discontinuities

Zijin Zhang Sergei Kamaletdinov Xiaofei Shi
Anton V. Artemyev Marco Velli Vassilis Angelopoulos

Solar wind plasma flow is characterized by intense, large-amplitude current sheets, also known as solar wind discontinuities. These regions are believed to play a crucial role in magnetic reconnection, solar wind ion heating, and energetic particle scattering. Although solar wind discontinuities share several properties with the classical MHD model of rotational discontinuities, they exhibit more complex characteristics that include many kinetic properties, going beyond this model. One of the most puzzling properties of these discontinuities is their Alvenicity, which describes the relationship between Alfvén and plasma velocity jumps across discontinuities. Although the high correlation of these jumps suggests the rotational nature of discontinuities, the significant differences in jump amplitudes indicate the necessity of kinetic mechanisms to describe the stress balance within discontinuities. Spacecraft observations show that plasma thermal anisotropy alone may not sufficiently explain this difference and achieve stress balance. In this study, we present a theoretical model in which this difference is explained by the kinetics of interpenetrating ion beams crossing the discontinuity. Our model successfully describes the observed properties of discontinuities within the inner heliosphere.

References

- Steinhauer et al. [2008]
- Artemyev et al. [2020]
- Neukirch et al. [2020]
- Vasko et al. [2014]

Introduction

1. Observation features of solar wind discontinuities
2. The necessity of kinetic models to describe solar wind discontinuities

3. Current theoretical models of solar wind discontinuities and their limitations

- Harris current sheet Harris [1962]

Observations of magnetic discontinuities exhibit Alfvenic properties, with the plasma velocity variation correlating well with magnetic field components variations. However, the amplitude of the plasma velocity jump is often significantly smaller than the Alfvén velocity jump, indicating a more complicated picture than the classical MHD model of rotational discontinuities. Figure 1 show observations of magnetic discontinuities in different regions of the heliosphere, PSP within 0.2 AU, Wind upstream of the Earth's bow shock, and ARTEMIS in the Earth's magnetotail. Previously, this discrepancy has been interpreted as a possible contribution of anisotropy that decreases the Alfvén velocity jump, or a discontinuity non-stationarity due to residual magnetic energy, or an ion nonadiabatic interaction with intense (thin) discontinuities that shapes the nongyrotropic ion distribution to include a nondiagonal term of the pressure tensor, with a cross-discontinuity gradient decreasing the Alfvén velocity jump Artemyev et al. [2020].

These differences could not be simply explained by the aniostropy of the plasma thermal pressure alone (assuming a Maxwellian distribution that fits both the parallel and perpendicular temperatures) and suggest that kinetic mechanisms are necessary to describe the stress balance within discontinuities.

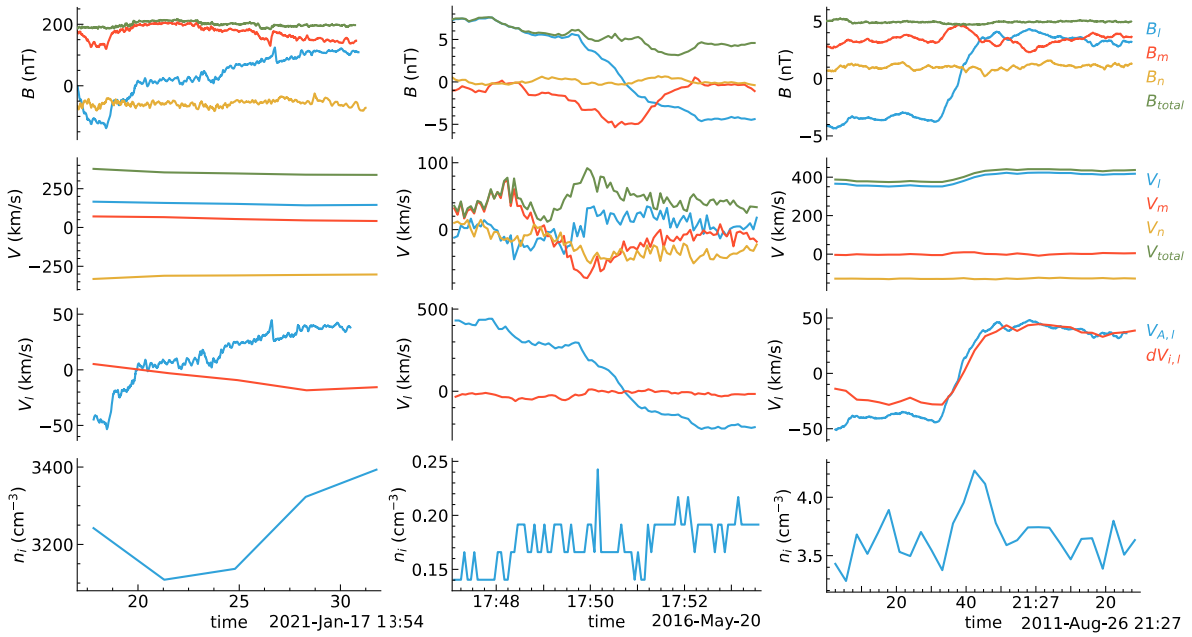

Figure 1: Three examples of solar wind discontinuities observed by Parker Solar Probe (PSP), ARTEMIS and Wind spacecraft with sub-Alfvenic flow velocity.

Force-free Harrison and Neukirch [2009] (A necessary condition on the pseudopotential plasma pressure to allow for force-free 1D VM equilibria is formulated.)

Multifluid Model

We used a steady-state multi-fluid model for assumed 1-D force-free current sheets. This approach, inspired by Steinhauer et al. [2008], has the advantage of being analytically tractable while providing the necessary complexity to include the kinetic effects of multiple ion species. Kinetic approach, which is in principle more accurate, is hard to solve analytically and difficult to interpret the measurements. The multifluid model is a good compromise between the simplicity of the MHD model and the complexity of the kinetic model. One disadvantage of the multifluid model, however, is that there are more unknowns than equations. This means that the model is underdetermined and requires additional assumptions to be solved. This closure problem is usually solved by choosing equations of state. In this study, we first attempted to solve the system with a scalar pressure model, but then the system was overdetermined and no solution was found. We avoid this problem by assuming a specific profile for one of the variables, which is then used to solve the rest of the system.

Plasma-Field Equations for Force-free current sheet

Following Steinhauer et al. [2008], we consider a one-dimensional force-free current sheet where $B_x^2+B_y^2 = B_0^2 = \text{const}$, with all variables dependent solely on z. The system comprises multiple steady-state ion species (fluid groups) and a background electron fluid.

Electron motion is along the field lines $\mathbf{u_e} = \Gamma_e \mathbf{B}/(n_e B_z)$. And the conservation of fluid mass $d(n_\alpha u_{\alpha z})/dz = 0$ integrate to a constant parameters $\Gamma_\alpha = n_\alpha u_{\alpha z}$. The momentum equations for each ion species are given by

$$\begin{aligned}
\Gamma_\alpha \frac{du_{\alpha x}}{dz} &= n_\alpha u_{\alpha y} B_z - \Gamma_\alpha B_y \\
\Gamma_\alpha \frac{du_{\alpha y}}{dz} &= \Gamma_\alpha B_x - n_\alpha u_{\alpha x} B_z \\
\Gamma_\alpha \frac{du_{\alpha z}}{dz} &= -\frac{1}{2}\frac{dp_\alpha}{dz} - n_\alpha \frac{d\phi}{dz} + n_\alpha u_{\alpha x} B_y - n_\alpha u_{\alpha y} B_x
\end{aligned} \tag{1}$$

Ampere's law connects the fields and the flow components

$$dB_y/dz = -J_x = -\sum_\alpha n_\alpha u_{\alpha x} + n_e u_{ex} = -n u_x + \Gamma_e B_x/B_z \tag{2}$$

$$dB_x/dz = J_y = \sum_\alpha n_\alpha u_{\alpha y} - n_e u_{ey} = n u_y - \Gamma_e B_y/B_z \tag{3}$$

$$dB_z/dz = J_z = \sum_\alpha n_\alpha u_{\alpha z} - n_e u_{ez} = n u_z - \Gamma_e \tag{4}$$

And the Gauss's law for magnetism gives another constant parameter $B_z = \text{const}$.

This is a system of $3N+2$ equations for $4N+2$ unknown dependent variables: B_x, B_y, and N each of n, p, u_x, and u_y. Since we are interested in force-free solutions with $B_x^2 + B_y^2 = B_0^2 = \text{const}$, this condition provides an additional equation for the system.

A scalar pressure model, which provides another N equations connecting p and n, was attempted as per Steinhauer et al. [2008], but no solution was found (the system was overdetermined). Therefore, the system is considered with free parameters. For a system with two ion species, there are 9 equations for 10 unknowns. The system can be solved by setting one of the parameters to have a specific profile and solving the rest of the system.

The force-free condition let us express the magnetic field in terms of the rotation angle θ as $B_x = B_0 \cos\theta$ and $B_y = B_0 \sin\theta$. From Ampere's law (Equation 2) and (Equation 3), we have:

$$n(u_x B_y - u_y B_x) = 0$$

And we could express the density and bulk velocity in terms of every ion species: $n_\alpha u_{\alpha x} B_y = n_\alpha u_{\alpha y} B_x + C_\alpha$. This above equation can be rewritten as $\sum_\alpha C_\alpha = 0$. The simplest case is to set $C_\alpha = 0$ for all species, which is the case we will consider in this study.

$$n_\alpha(u_{\alpha x} B_y - n_\alpha u_{\alpha y} B_x) = 0 \tag{5}$$

Combining the above equation with the first two equations in (Equation 1), we have:

$$u_{\alpha x}^2 + u_{\alpha y}^2 = const$$

This would let us express the bulk velocity in terms of the rotation angle θ_α as $u_{\alpha x} = u_\alpha \cos\theta_\alpha$ and $u_{\alpha y} = u_\alpha \sin\theta_\alpha$. And substituting the above expression into the our assumption (Equation 5), we have:

$$\tan\theta = \tan\theta_\alpha$$

#TODO# Here we consider the case where $\theta_\alpha = \theta$ for all species, but the same procedure can be applied to the case where $\theta_\alpha = \theta + \pi$ and it would give the same results.

The first momentum equation (Equation 1) after substituting the above expression becomes:

$$-u_\alpha \sin\theta_\alpha \theta'_\alpha = n_\alpha u_\alpha \sin\theta_\alpha B_z/\Gamma_\alpha - B_0 \sin\theta$$

$$\Rightarrow \theta'_\alpha = -\frac{n_\alpha B_z}{\Gamma_\alpha} + \frac{B_0}{u_\alpha} \tag{6}$$

Note that θ_α, n_α are dependent variables, and $u_\alpha, B_0, B_z, \Gamma_\alpha$ are constants pre-determined by the system. So given the profile of n_α and the boundary condition, we could solve the above equation to get the profile of θ_α, thus the profile of u_α.

The Ampere's law (Equation 3) after substitution becomes:

$$-B_0 \sin\theta\theta' = \sum n_\alpha u_\alpha \sin\theta_\alpha - \Gamma_e B_0 \sin\theta/B_z$$

$$\Rightarrow \theta' = -\frac{\sum n_\alpha u_\alpha}{B_0} + \frac{\Gamma_e}{B_z} \tag{7}$$

The above equation relates the rotation angle θ to the plasma bulk velocity $nu \equiv \sum n_\alpha u_\alpha$. By equating the above two equations of θ', we could get a equation relating the plasma bulk velocity to one specific species:

$$nu = B_0 \left(\frac{\Gamma_e}{B_z} + \frac{n_\alpha B_z}{\Gamma_\alpha} - \frac{B_0}{u_\alpha} \right)$$

In the asymptotic region, as all variables approach constant values, the derivatives must vanish. For Equation 6, this means $\theta_\alpha(\infty)' = 0 = -\frac{n_\alpha(\infty)B_z}{\Gamma_\alpha} + \frac{B_0}{u_\alpha}$. This relates the velocity of each species to the asymptotic density. Rewriting the Equation 6 in terms of asymptotic values, we have:

$$\theta'_\alpha = \frac{B_z}{\Gamma_\alpha}(n_\alpha - n_\alpha(\infty)) \tag{8}$$

Conveniently, the center of the current sheet is chosen as the origin $z = 0$, which corresponds to the lower boundary of Equation 6. As a result, the boundary condition for the rotation angle is given by $\theta_\alpha(0) = \pi/2$.

Combine momentum equation (x) (Equation 1) and Ampere's law (y) (Equation 3) with condition that the constant of integration vanishes at the current sheet center yield

$$B_x B_z = \sum n_\alpha u_{\alpha,x} u_{\alpha,z} = \sum \Gamma_\alpha u_{\alpha,x}$$

Evaluate the above equation in the asymptotic limit, we have

$$B_z{}^2 = \sum \Gamma_\alpha^2 / n_\alpha(\infty) \tag{9}$$

To simplify the analysis, it is useful to employ a dimensionless system by normalizing the variables with their asymptotic values: in this study, the magnetic field is normalized by $B_{\text{ref}} = B_z$, and the density is normalized by $n_{\text{ref}} = n(\infty)$. Other reference values derived from these two are displayed in the table below.

Variable	Reference Value
Frequency (ion plasma frequency)	$\omega_{pi} = \sqrt{\frac{n_{\text{ref}} e^2}{m_i \varepsilon_0}}$
Length (ion inertial length)	$L_{\text{ref}} = c/\omega_{pi}$
Velocity (Alfvén velocity)	$V_{\text{ref}} = B_{\text{ref}}/\sqrt{\mu_0 m_i n_{\text{ref}}}$

Results

The multifluid model developed above is used here to study a specific example and the effects of model parameters: assume a density profile for one species taking the form of a Gaussian function

$$n_1(z) \to n_1(\infty)\left(\frac{c_1}{\frac{z}{\delta_1}^2 + 1} + 1\right)$$

Solving the Equation 8 analytically, we have the rotation angle profile as

$$\theta(z) \to \frac{\pi\Gamma_1 - 2c_1\delta_1 B_z n_1(\infty)\tan^{-1}\left(\frac{z}{\delta_1}\right)}{2\Gamma_1}$$

For the simplest situation where we have two group of ions of the same density but opposite bulk velocity, i.e., $n_1 = n_2, u_1 = -u_2$, the system could be determined given c_1, δ_1, and B_0. The system profile of magnetic field, plasma density, and plasma velocity for one specific case ($\delta_1 = 1, c_1 = 1/\sqrt{2}, B_0 = 2$) is plotted below Figure 2. The specific profiles are chosen to have zero electron current across the current sheet and zero B_y in the asymptotic limit, corresponding to a 180° rotation of the magnetic field across the current sheet. However, in general, we would expect the electron current to be non-zero.

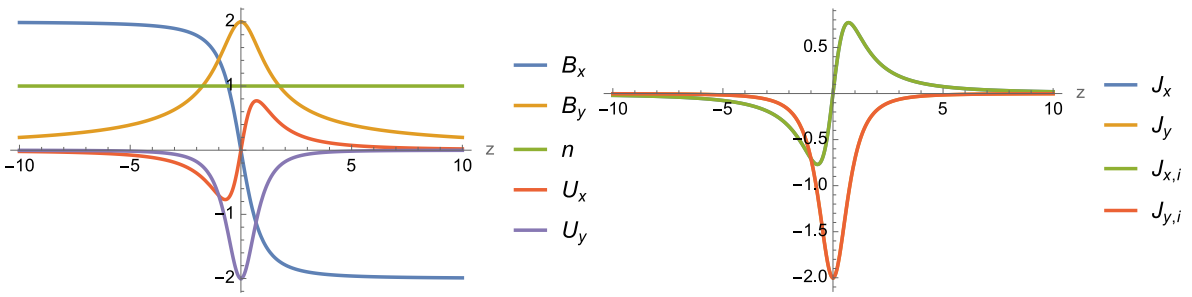

Figure 2: (a). Magnetic field, ion density, and ion bulk velocity for $n_1 = n_2, u_1 = -u_2$ and $\delta_1 = 1, c_1 = 1/\sqrt{2}, B_0 = 2$. (b). Current density profiles for the same case.

Alfvenicity

For the same asymptotic magnetic field, it is interesting to see how the plasma profiles change with different system parameters.

Here we set $B_y(z = \infty) = 1/2B_0, B_0 = 2B_z$, and let two ion species have the opposite bulk velocity but this time with different densities. By varying $n_1(\infty)$, we find that the magnetic field profiles are exactly the same, while plasma density and velocity profiles vary.

We normalize the plasma velocity by asympotic Alfvén velocity $v_A(\infty) = B_0/\sqrt{\mu_0 m_i n}$, and the profiles are plotted below Figure **??**. It could be seen that for $n_1(\infty) = 0.5$, we have zero bulk velocity change across the current sheet in the asymptotic limit. And the change of bulk velocity across the current sheet increases with $n_1(\infty)$ decreasing to zero Figure 3b. The normalized plasma velocity U_y in the aympotic limit decreases with $n_1(\infty)$ decreasing to zero Figure 3c.

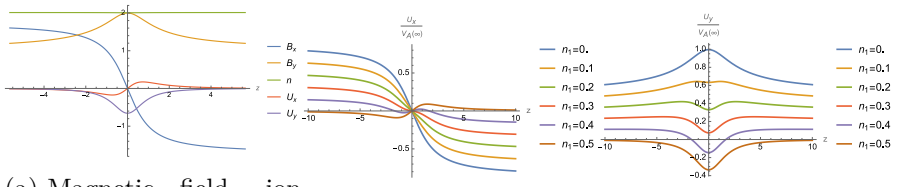

(a) Magnetic field, ion density, and ion bulk velocity for two ion species with same bulk velocity but different densities.

(b) Plasma velocity U_x profiles normalized by aysmpotic Alfvén velocity for different $n_1(\infty)$.

(c) Plasma velocity U_y profiles normalized by aysmpotic Alfvén velocity for different $n_1(\infty)$.

Normalized by Alfvén velocity $v_{A,x}$ and $v_{A,y}$, the plasma velocity profiles are plotted below Figure 4a and Figure 4b. The normalized plasma velocity profiles are exactly the same for $U_x/v_{A,x}$ and $U_y/v_{A,y}$ for same $n_1(\infty)$. When $n_1(\infty)$ decreases to zero, the normalized plasma velocity would approach one in the asymptotic limit, indicating the Alvenicity of the current sheet.

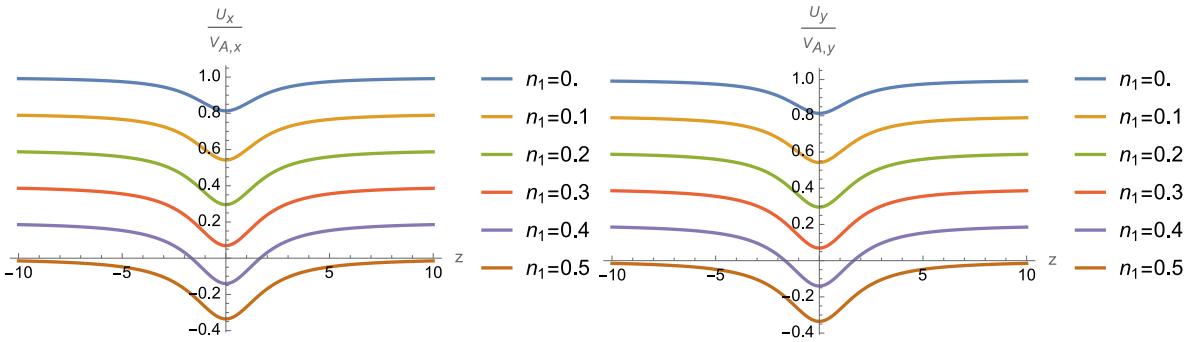

(a) Plasma velocity U_x profiles normalized by $v_{A,x}$ for different $n_1(\infty)$.

(b) Plasma velocity U_y profiles normalized by $v_{A,y}$ for different $n_1(\infty)$.

The asymptotic velocity for the each species, bulk velocity and normalized one by Alfvén velocity are plotted below Figure 5 and Figure 5b for the case of $\lambda_{z,2} = -1$ (two groups of opposite velocity in z direction) and $\lambda_{z,2} = -1/2$ respectively. For the case of $\lambda_{z,2} = -1$ as shown in Figure 5a, the normalized velocity reaches zero when $n_1(\infty) = 0.5$. The bulk velocity of each species is the same in the asymptotic limit and does not depend on $n_1(\infty)$. However, this does not generally hold when $\lambda_{z,2} \neq -1$ as shown in Figure 5b for the case of $\lambda_{z,2} = -1/2$.. The normalized velocity reaches zero when $n_1(\infty) = 1/3$, and the bulk velocity of each species differs in the asymptotic limit and depends on $n_1(\infty)$.

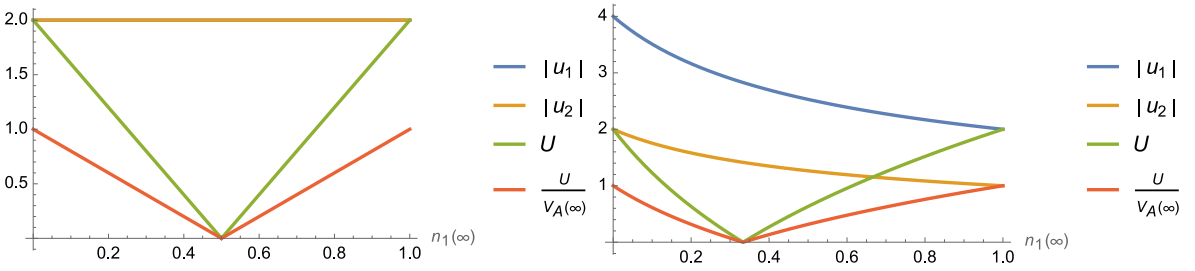

(a)

(b)

Figure 5: Asymptotic velocity for each species, bulk velocity and normalized one by Alfvén velocity for the case of $\lambda_{z,2} = -1$ (a) and $\lambda_{z,2} = -1/2$ (b).

Current Sheet Thickness

TODO: define and compare current sheet thickness

TODO: compare with Harris current sheet solution with same thickness

Density Peaking

Summary

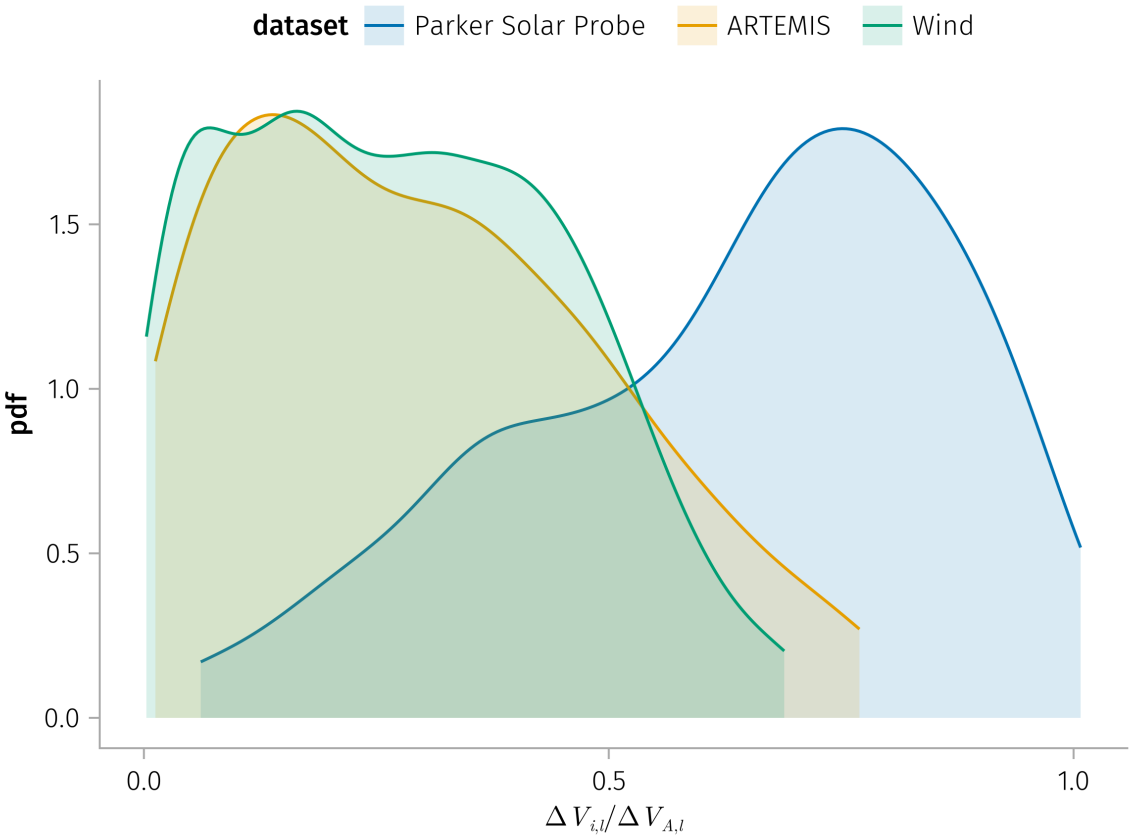

Figure 6: Statistics of the asymptotic velocity ratio from PSP, Wind, and ARTEMIS spacecraft observations during PSP encounter 7 period from 2021-01-14 to 2021-01-21.

References

Anton V. Artemyev, Vassilis Angelopoulos, Ivan Y. Vasko, and Lev M. Zelenyi. Ion Nongyrotropy in Solar Wind Discontinuities. *The Astrophysical Journal Letters*, 889(1):L23, January 2020. ISSN 2041-8205. doi: 10.3847/2041-8213/ab6b2e.

E. G. Harris. On a plasma sheath separating regions of oppositely directed magnetic field. *Il Nuovo Cimento (1955-1965)*, 23(1):115–121, January 1962. ISSN 1827-6121. doi: 10.1007/BF02733547.

M. G. Harrison and T. Neukirch. Some remarks on one-dimensional force-free Vlasov–Maxwell equilibria. *Physics of Plasmas*, 16(2):22106, February 2009. ISSN 1070-664X. doi: 10.1063/1.3077307.

T. Neukirch, I. Y. Vasko, A. V. Artemyev, and O. Allanson. Kinetic Models of Tangential Discontinuities in the Solar Wind. *Astrophysical Journal*, 891(1):86, March 2020. ISSN 0004-637X. doi: 10.3847/1538-4357/ab7234.

L. C. Steinhauer, M. P. McCarthy, and E. C. Whipple. Multifluid model of a one-dimensional steady state magnetotail current sheet. *Journal of Geophysical Research: Space Physics*, 113(A4), 2008. ISSN 2156-2202. doi: 10.1029/2007JA012578.

I. Y. Vasko, A. V. Artemyev, A. A. Petrukovich, and H. V. Malova. Thin current sheets with strong bell-shape guide field: Cluster observations and models with beams. *Annales Geophysicae*, 32(10):1349–1360, October 2014. ISSN 0992-7689. doi: 10.5194/angeo-32-1349-2014.